J Ind Microbiol Biotechnol (2013) 40:697–704
DOI 10.1007/s10295-013-1268-4

FERMENTATION, CELL CULTURE AND BIOENGINEERING

Enhanced thermostability of keratinase by computational design and empirical mutation

Baihong liu · Juan Zhang · Zhen Fang · Lei Gu · Xiangru Liao · Guocheng Du · Jian Chen

Received: 10 January 2013 / Accepted: 1 April 2013 / Published online: 26 April 2013

Abstract Keratinases are proteolytic enzymes capable of degrading insoluble keratins. The importance of these enzymes is being increasingly recognized in fields as diverse as animal feed production, textile processing, detergent formulation, leather manufacture, and medicine. To enhance the thermostability of *Bacillus licheniformis* BBE11-1 keratinase, the PoPMuSiC algorithm was applied to predict the folding free energy change ($\Delta\Delta G$) of amino acid substitutions. Use of the algorithm in combination with molecular modification of homologous subtilisin allowed the introduction of four amino acid substitutions (N122Y, N217S, A193P, N160C) into the enzyme by site-directed mutagenesis, and the mutant genes were expressed in *Bacillus subtilis* WB600. The quadruple mutant displayed synergistic or additive effects with an 8.6-fold increase in the $t_{1/2}$ value at 60 °C. The N122Y substitution also led to an approximately 5.6-fold increase in catalytic efficiency compared to that of the wild-type keratinase. These results provide further insight into the thermostability of keratinase and suggest further potential industrial applications.

Keywords Keratinase · PoPMuSiC · Thermostability · Site-directed mutagenesis · *Bacillus licheniformis*

B. liu · J. Zhang (✉) · Z. Fang · L. Gu · X. Liao
Key Laboratory of Industrial Biotechnology, Ministry of Education, Jiangnan University, Wuxi 214122, China
e-mail: zhangj@jiangnan.edu.cn

B. liu
e-mail: liu8bai6hong@163.com

B. liu · J. Zhang · Z. Fang · L. Gu · X. Liao · G. Du · J. Chen
School of Biotechnology, Jiangnan University, Wuxi 214122, China

G. Du
The Key Laboratory of Carbohydrate Chemistry and Biotechnology, Ministry of Education, Jiangnan University, Wuxi 214122, China

J. Chen (✉)
National Engineering Laboratory for Cereal Fermentation Technology, Jiangnan University, Wuxi 214122, China
e-mail: jchen@jiangnan.edu.cn

Introduction

Keratin is an insoluble and fibrous structural protein that is a constituent of feathers and wool. The protein is abundantly available as a by-product from keratinous wastes, representing a valuable source of proteins and amino acids that could be useful for animal feeds or as a source of nitrogen for plants [10]. However, keratin-containing wastes have high mechanical stability and are difficult to degrade by common proteases.

Keratinases are specialized proteolytic enzymes that degrade keratins; most are classified as serine- or metalloproteases. Keratinases have been isolated and purified from different bacteria, actinomycetes, and fungi [3]. Cloning and expression of keratinase genes in a variety of expression systems have also been reported [9]. Recently, we cloned the *ker* gene encoding *Bacillus licheniformis* BBE11-1 keratinase and expressed the gene in *Bacillus subtilis* WB600 under the strong P_{HpaII} promoter harbored in the pMA0911 vector [13]. However, the keratinase was completely denatured after a 30-min exposure to 60 °C, which limits the application of this enzyme. Thermostable enzymes that would function at higher reaction temperatures would decrease the possibility of microbial

contamination, promote the disorganization of raw materials, and improve enzyme penetration [25]. The higher operation temperature that would be possible using a thermostable keratinase is clearly advantageous because of a higher reactivity (higher reaction rate and lower diffusional restrictions), enhanced stability, and higher process yield (increased solubility of substrates and products and favorable equilibrium displacement in endothermic reactions).

The PoPMuSiC algorithm is a web server that predicts the thermodynamic stability changes caused by single site mutations in proteins, using a linear combination of statistical potentials whose coefficients depend on the solvent accessibility of the mutated residue. PoPMuSiC has a good prediction performance, with a correlation coefficient of 0.8 between the predicted and measured stability changes in cross validation, after exclusion of 10 % outliers [7]. Moreover, it is very fast, allowing the prediction of the stability changes resulting from all possible mutations in a medium-size protein in less than a minute. It has proved useful in the design of stabilized point mutations of tobacco etch virus protease [5, 23], pyruvate formate lyase [23] and feruloyl esterases [26]. PoPMuSic evaluates the stability changes resulting from all possible mutations and returns a report containing a list of the most stabilizing mutations or destabilizing mutations, or the mutations that do not affect stability. Stabilizing mutations (except the active site) can then be chosen for further testing. On the other hand, we noticed that the *B. licheniformis* BBE11-1 keratinase has high homology compared with subtilisin E (75.4 %) and subtilisin BPN′ (74.9 %) (Fig. 1), two enzymes that have been intensively studied to improve their thermostability [4, 15, 16, 18, 24, 27]. Asn218Ser [4] was generated by random mutagenesis in subtilisin BPN′; the mutant displayed a 20-fold increase in the $t_{1/2}$ value at 65 °C. The Ser161Cys mutation [18] in subtilisin E produced a 2.9-fold increase in the $t_{1/2}$ value at 60 °C. Directed evolution analyses [27] showed that Ser194Pro and Gly166Arg were stabilizing mutations in subtilisin E. These empirical mutations could be an excellent guide and a useful supplement in the PoPMuSiC algorithm to enhance the thermostability of keratinase.

In this study, PoPMuSiC-2.1 was applied to predict the thermostability of keratinase from *B. licheniformis* BBE11-1. The effects of three amino acid substitutions were experimentally investigated. One mutant, N122Y, increased the thermostability and catalytic efficiency of keratinase. Combined with three other previously-described mutations from subtilisin E and subtilisin BPN′ (N160C, A193P, N217S), the four amino acid substitutions provide the means to enhance keratinase thermostability.

Materials and methods

Bacterial strains, plasmids and materials

The strain *B. subtilis* WB600 and the vector pMA5 [28] were used for the expression of keratinase. *Bacillus licheniformis* BBE11-1 (GenBank accession no. JQ894491) was used as the source of genomic DNA. *Escherichia coli* JM109 purchased from TaKaRa (Dalian, China) was used as the host for plasmid construction. The pMD19-T vector used for *ker* gene cloning was purchased from TaKaRa (Dalian, China). PrimeSTAR HS DNA polymerase, restriction endonucleases, PCR reagents, Genomic Extraction Kit and MutanBEST kit used for site-directed mutagenesis were purchased from TaKaRa (Dalian, China). DNA sequencing was performed by Sangon (Shanghai, China). Keratin (from wool) used as a substrate was purchased from J&K (Beijing, China). Folin-Ciocalteu's phenol reagent was purchased from Sangon (Shanghai, China). All other chemicals and reagents were of analytical grade. The *N*-succinyl-L-Ala-Ala-Pro-Phe-p-nitroanilide (AAPF) was purchased from Sigma-Aldrich (Shanghai, China).

Selection and construction of point mutations

Homology modeling of wild-type and mutant keratinase (Fig. 2a) from *B. licheniformis* BBE11-1 was performed using the crystal structure of *B. licheniformis* strain Subtilisin Carlsberg (PDB 3unxA, 1.26 Å resolution) [8] as the template by the SWISS-MODEL protein-modeling sever (http://swissmodel.expasy.org/) [1]. The models had 99.27 % sequence identity with the template. We used the PoPMuSiC-2.1 algorithm to search for amino acid substitutions that could possibly improve the thermostability of keratinase. The active sites were not allowed to be changed by the algorithm. Based on the values of the folding free energy change (ΔΔG) predicted by the PoPMuSiC algorithm, the amino acid substitutions were predicted to have the most stabilizing effect and the corresponding mutations were introduced into *Ker* by site-directed mutagenesis. Meanwhile, the other four mutations (Asn217Ser, Ala193Pro, Asn160Cys, Gly165Arg) that appreciably enhanced the thermostability of subtilisin E and subtilisin BPN′ were also introduced into *Ker* by site-directed mutagenesis. The number of hydrogen bonds in the enzyme was calculated by Discovery Studio 2.5 (Fig. 2).

Site-directed mutagenesis

Site-directed mutagenesis was performed using the MutanBEST kit. The one-step PCR method was carried out by

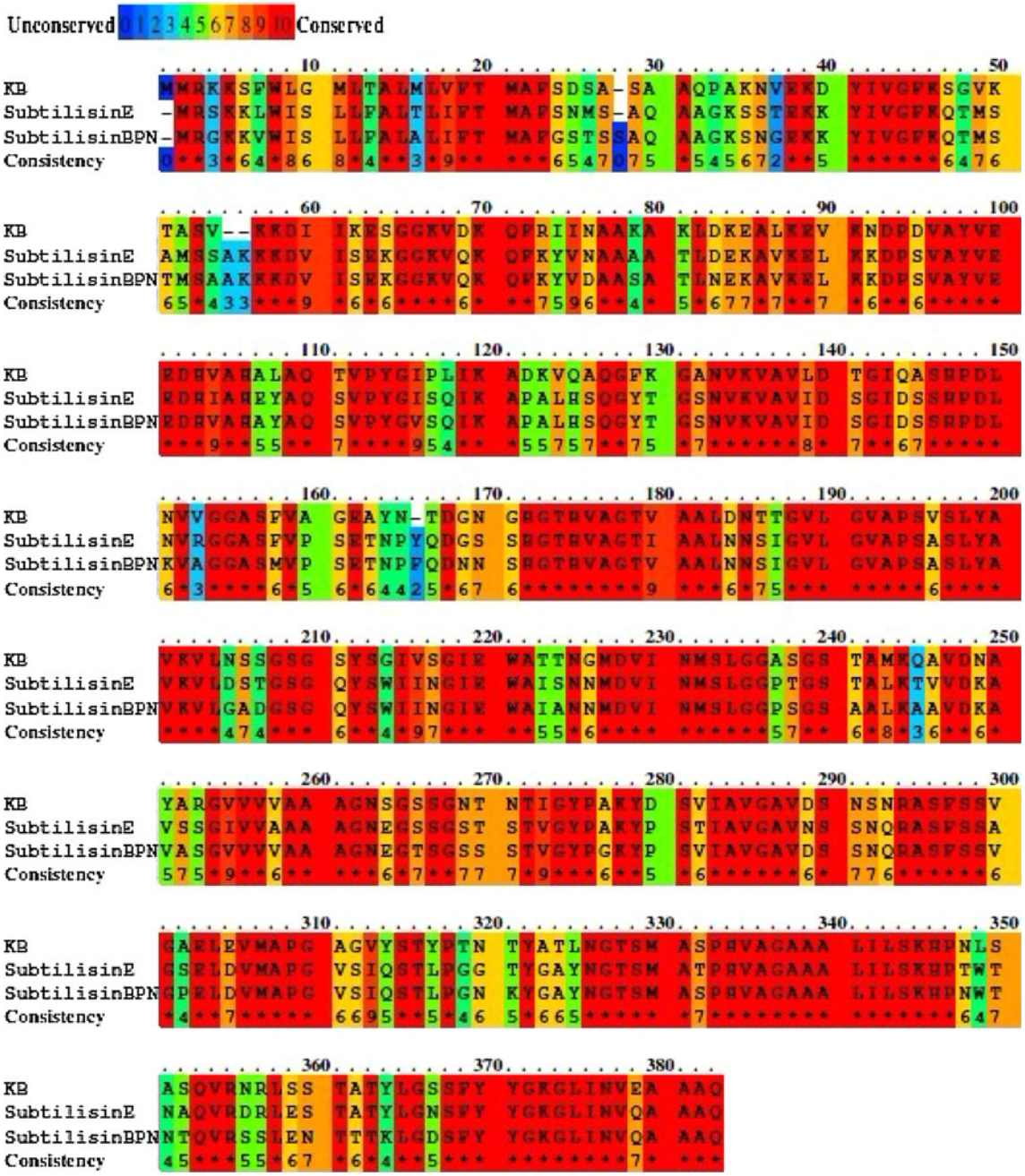

Fig. 1 Protein sequence alignment of keratinase from *B. licheniformis* BBE11-1 (KB), subtilisin E and subtilisin BPN′ by PRALINE. Amino acid sequence alignment was performed by PSI-BLAST pre-profile processing (Homology-extended alignment) available from the PRALINE online resource portal (http://www.ibi.vu.nl/programs/pralinewww/)

PrimeSTAR HS DNA polymerase using the plasmid *ker*/pMD19-T as the template DNA and oligonucleotide primers. The sequences of the mutagenic primers are shown in Supplementary materials (Table 1). The PCR products were treated with blunting kination enzyme and Ligation Solution I (TaKaRa, Dalian, China), ligated into circular plasmids, and then transformed into *E. coli* JM109. The successful introductions of the desired mutations were confirmed by DNA sequencing.

Construction of expression vector

Ker was amplified for the pMD 19-T-keratinase vector and the *Nde* I and *Bam* HI cloning sites were introduced into the primers to permit ligation into the pMA5 vector. The 5′ primer was 5′-GGAATTCCATATGATGAGGAAAAAGA GTTTTTGG and the 3′ primer was 3′-CGCGGATCCT-TATTGAGCGGCAGCTTCG. The ligation mixture was used to chemically transform competent *E. coli* JM109.

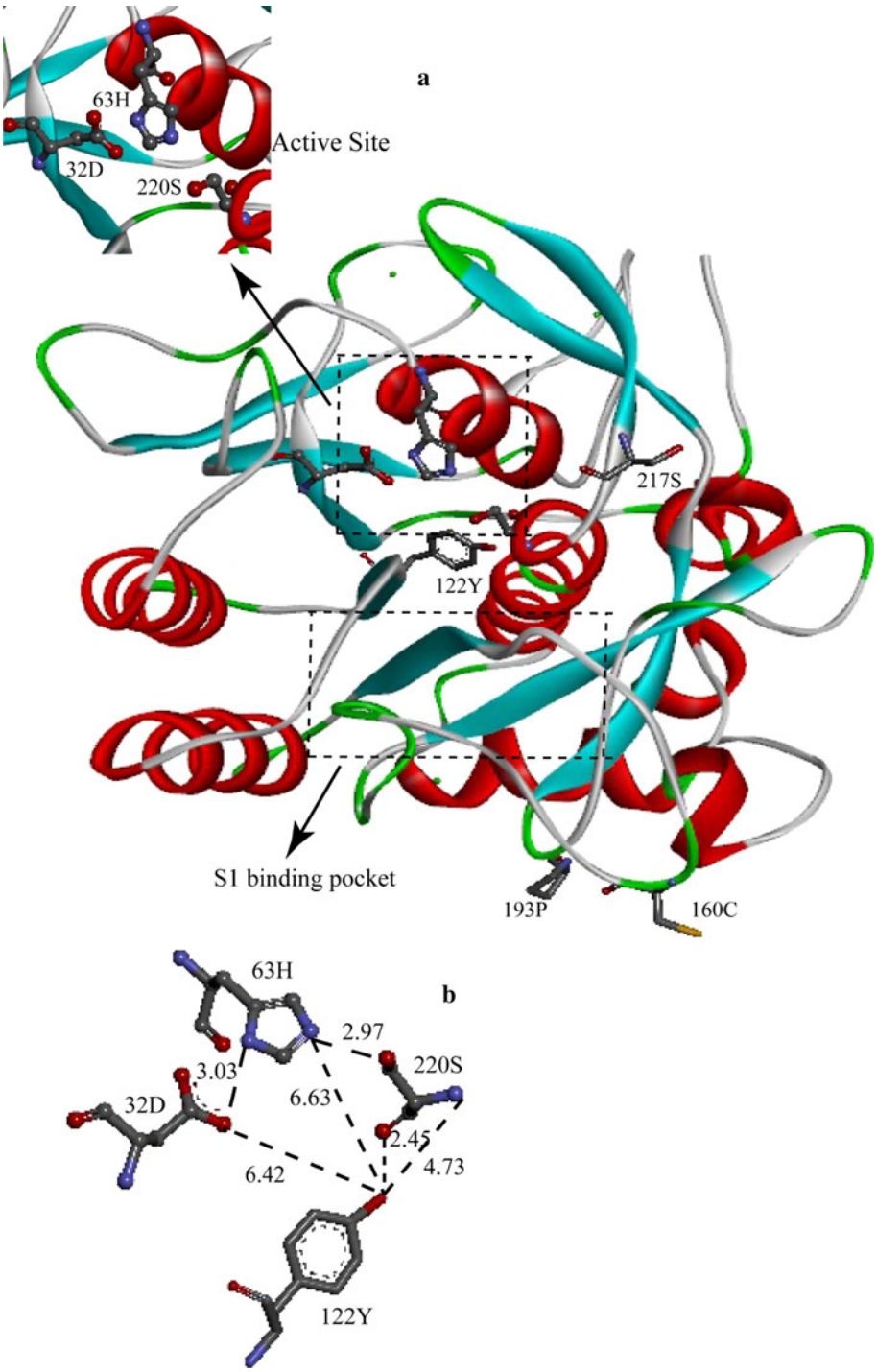

Fig. 2 The model structure of keratinase, local model of the mutation sites and the catalytic residues in keratinase (**a**). The model structure of keratinase was constructed with the crystal structure of Subtilisin Carlsberg (PDB 3unxA, 1.26 Å resolution). The α helices and β sheets are shown in red and cyan, respectively. The active site (Asp32, His63, 220Ser) is shown in "Ball and stick" representation. The mutant positions are shown in "sticks". S1 binding pocket: a distinct, large and elongated cleft, surrounded at the sides and bottom by the backbone segments 124–127 and 151–154, at the bottom end by residue 165 and at the rim by residues 155 and 128 [17]. The distances (Å) from the Tyr122 to active site (Asp32, His63, 220Ser) in keratinase are shown (**b**). The oxygen atoms are in *red*, the nitrogen atoms in *light blue*, the carbon atoms in *yellow green*, and the sulfur atoms in *yellow* (color figure online)

The plasmids isolated from these transformants were confirmed by DNA sequencing and the plasmid with the correct sequences was designated pMA5-*ker*. *Bacillus subtilis* WB600 was chosen as the host and was transformed by the pMA5-*ker* plasmid. After 12 h of incubation at 37 °C on LB agar containing 20 μg/mL kanamycin, transformants were confirmed by colony PCR and DNA sequencing, and were used for further expression and purification.

Expression, purification of keratinase

To confirm the expression of keratinase, the different mutated transformants with pMA5-*ker* plasmids were cultured in a 250 mL shake flask containing fermentation medium (yeast extract, 5 g/L; peptone, 10 g/L; NaCl, 10 g/L; glucose, 10 g/L; $MgSO_4$, 0.1 g/L) at 37 °C for 48 h. The culture broth was centrifuged at 8,000×*g* for 10 min, and

Table 1 Oligonucleotide primers used for site-directed mutagenesis

Directed mutation	Nucleotide sequence (5′ → 3′)[a]
Asn122Tyr	GATGTTATCAAT(TAC)ATGAGCCTTGGG
Gly177Cys	GCTGTTGGT(TGC)GCGGTAGACTCT
Gly201Trp	CTCCTGGC(TGG)GCAGGCGTATAC
Asn217Ser	CATTGAAC(TCA)GGAACGTCAATGGC
Ala193Pro	GTGGGAGAC(CCA)GAGCTTGAAGTCA
Asn160Cys	CTTCAGGAAAC(TGC)ACGAATACAATTG
Gly165Arg	CAATTGGC(CGT)TATCCTGCGAAATAC

[a] Nucleotides underlined correspond to the codons chosen for mutation. Nucleotides in parentheses replace the underlined nucleotides

the keratinase was concentrated by ultrafiltration using 10 kDa membrane (Pellicon® XL filter; Millipore corporation, USA). The enzyme solution was then injected into the AKTA purifier (GE Healthcare, USA) through Phenyl Sepharose Fast Flow columns (5 mL) for hydrophobic interaction chromatography (*HIC*) (GE Healthcare, USA). After eluting the unbound proteins, a gradient elution was performed using ammonium sulfate (from 1 to 0 M), and the fractions were collected for the activity assay and SDS-PAGE analysis.

Determination of enzymatic activity and kinetic parameters

The keratinase activity was determined according to the modified method of Yamamura et al. [22]. A portion (0.5 mL) of the enzyme solution was incubated with 1.5 mL of 1 % keratin in 50 mM Gly/NaOH buffer (pH 10.5) at 40 °C for 15 min. The reaction was terminated with 2 mL of 6 % trichloroacetic acid (TCA), and then allowed to stand for 10 min. After centrifugation (Tomy MRX-152, Japan) (15,000×*g*; 10 min), the supernatant (0.5 mL) was mixed with Bradford reagent (1:1 dilution) and 2.5 mL of 0.5 M Na_2CO_3 at 40 °C for 15 min. The keratinase activity was measured at 660 nm with a spectrophotometer (Beckman DU640, USA), and expressed in keratin units. One unit is defined as an increase of 0.01 OD value at 660 nm in 15 min.

The thermal inactivation half-life ($t_{1/2}$) at 60 °C was determined by the residual keratinase activity versus incubation time that was deduced by linear regression [21]. The half-inactivation temperature (T_{50}) was defined by the temperature at which the enzyme lost 50 % activity, when the purified enzymes were incubated at temperatures ranging from 58 to 68 °C (1 °C interval) for 10 min.

The kinetic parameters including K_m and V_{max} were calculated from a double reciprocal (Lineweaver–Burk) plot [12] using synthetic peptides of AAPF in a concentration range of 100–600 mM at 40 °C in assay buffer containing 50 mM glycine-NaOH (pH 10.5).

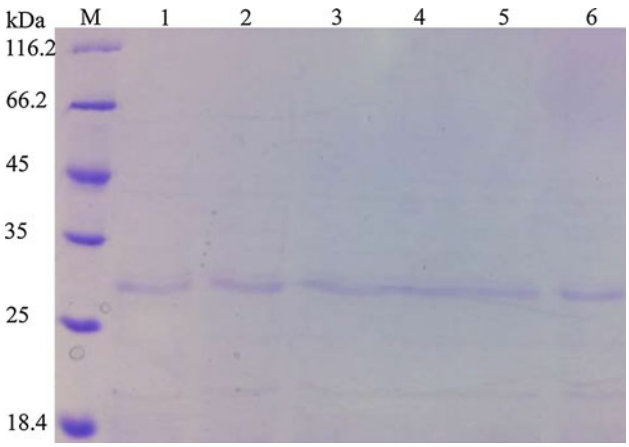

Fig. 3 SDS-PAGE of purified wild-type and mutant keratinase. *Lane M* molecular weight marker; *lanes 1–6* wild-type, N122Y, N160C, A193P, N217S, N122Y/N160C/A193P/N217S

Results and discussion

Identification of stabilizing residues and expression of mutants in *B. subtilis*

According to the PoPMuSiC algorithm tool, all possible stabilizing point mutations in the keratinase were displayed based on the differences in folding free energy between the wild-type and mutant proteins. The three most stabilizing point mutations (Asn122Tyr, Gly177Cys, Gly201Trp) were chosen based on an Internet search. The evaluation of folding free energy changes calculated in silico caused by Asn122Tyr, Gly177Cys, and Gly201Trp single-site mutation was −2.33, −1.39, and −1.47 kcal/mol, respectively. All the mutants (Asn122Tyr, Gly177Cys, Gly201Trp, Asn217Ser, Ala193Pro, Asn160Cys, and Gly165Arg) were transformed into *B. subtilis* WB600 and expressed at the aforementioned conditions. Sodium dodecyl sulfate–polyacrylamide gel electrophoresis (Fig. 3) revealed a major protein band of about 30 kDa after purified (Table 2), consistent with that of our previous report [13].

Characterization of keratinase mutants

The wild-type and mutant keratinases were purified and their thermostability was tested. The G165R, G177C, and G201 W mutations were the neutral to wide-type and had half-lives of thermal inactivation ($t_{1/2}$) of approximately 9.0 min at 60 °C (Table 3). However, the other four amino acid substitutions (N217S, A193P, N160C, and N122Y) enhanced the thermostability of keratinase (Table 4). Of

Table 2 Purification of recombinant keratinase

Fraction	Protein (mg)	Specific activity (U/mg)	Yield (%)	Purification (fold)
Supernatant	140	2285.71	100	1.0
10 kDa cutoff	110	4818.18	50	2.1
Phenyl sepharose FF	50	9560.22	50	4.2

Table 3 Thermostability of wild-type keratinase and mutants predicted by the PoPMuSiC algorithm

Keratinase	ΔΔG[a] (kcal/mol)	$t^{b}_{1/2}$ (min)	T^{c}_{50} (°C)
Wild-type	–	9 ± 0.2	59
N122Y	−2.33	23 ± 0.3	62
G177C	−1.39	9 ± 0.2	59
G201 W	−1.47	10 ± 0.2	59

[a] Folding free energy changes between wild-type and variants were estimated with the PoPMuSiC algorithm

[b] Half-life of thermal inactivation at 60 °C was measured

[c] Half-inactivation temperature was measured after heat treatment for 10 min at 58–68 °C

Table 4 Thermostability of wild-type keratinase and variants

Keratinase	$t^{a}_{1/2}$ (min)	T^{b}_{50} (°C)
Wild-type	9 ± 0.2	59
N217S	19 ± 0.5	61
A193P	14 ± 0.7	60
N160C	16 ± 0.3	61
N217S/A193P/N160C	38 ± 1.1	63
N217S/A193P/N160C/N122Y	78 ± 1.5	66

[a] Half-life of thermal inactivation at 60 °C was measured

[b] Half-inactivation temperature was measured after heat treatment for 10 min at 58–68 °C

these mutations, the N122Y substitution mutant best enhanced the half-life time at 60 °C, from 9 to 23 min. Moreover, the half-inactivation temperature (T_{50}) for this mutant enzyme was increased by 3 °C. The N217S, A193P, and N160C substitutions did not substantially enhance thermostability, similar to previous reports [18, 27], and produced an enzyme half-life that was 1.5–2.1 times higher than the half-life of the wild-type enzyme. Combination studies with the four beneficial substitutions (N122Y, N217S, A193P, N160C) demonstrated that the corresponding quadruple mutant displayed synergistic or additive effects with an 8.6-fold increase in the $t_{1/2}$ value at 60 °C.

Keratinase from *B. licheniformis* belongs to the subtilisin family (>64 % identity with subgroups of true subtilisins) with the essential catalytic triad residues (D32, H63, S220) [17]. After the structural basis of thermostability from subtilisin was systematically studied, the reasons for the enhancement of thermostability caused by mutants could be empirically explained. According to the model, the N217S, A193P, N160C, and G165R mutations are located on the protein surface. G165R is located at the bottom region of the distinct, elongated cleft known as the S1 pocket, and is partially exposed. No activity was detected in the G165R substitution, but this mutant in subtilisin E (G166R) stabilized the enzyme [27]. N217S presumably increases thermostability by improving hydrogen bonding parameters of the 201–218 β-pair, as this substitution allows the anti-parallel strands to move closer together, allowing slightly shorter and stronger hydrogen bonds. Such a thermostabilizing mechanism was found in subtilisin BPN′ (N218S) [4]. The A193P mutation probably reduces the entropy of the flexible loop. Earlier research showed that thermophilic and extremely thermophilic enzymes have more proline residues in their loop/coils than does a mesophilic enzyme [2]. Introduction of proline at an appropriate site, such as the second sites of β turns, first turns of α helices, and the flexible loops in proteins, could improve protein thermostability [20]. Sequence comparisons of subtilisins from mesophilic and hyperthermophilic organisms detected mutation N160C only in a mesophilic enzyme from *Drosophila melanogaster*. However, how a single-Cys mutant enzyme enhanced the thermostability is unclear (Table 4).

Thermostability is associated with an increase in the packing density of the hydrophobic core and a decrease in internal cavities [6]. Residue 122 is located in the β4 sheet approximately 6 Å from the Asp32, His63, and Ser220 triad of catalytic residues. One of the possible causes of this thermostability is the higher hydrophobicity of tyrosine compared to asparagine, an additional aromatic residue compared with asparagines, which could contribute to a more compact core. To further explain the reasons for the enhanced thermostability by multiple substitutions, we used the PIC server (http://pic.mbu.iisc.ernet.in/index.html) and Discovery Studio 2.5 software to analyze intramolecular interactions of the wild type and mutant type. The PIC is a program that reveals canonical interactions such as hydrogen bonds, hydrophobic interactions, and electrostatic interactions that are well known as the dominant structural factors responsible for protein thermostability [19]. Although N122Y, A193P, S160C and N217S displayed reduced ionic interactions compared with the wild type enzyme, the substitutions could result in the addition of six new putative hydrophobic interactions, one new putative cation-pi interactions, and 11 new putative hydrogen bonds. Among them, N122Y added three new putative hydrophobic interactions. An earlier report

Table 5 Kinetic parameters of purified wild-type and mutant enzymes for hydrolysis of synthetic peptide

Keratinase	K_m (mM)	k_{cat} (s^{-1})	k_{cat}/K_m (s^{-1} mM^{-1})
Wild-type	2.42 ± 0.22	22.61 ± 1.98	9.34
N122Y	1.84 ± 0.14	96.7 ± 4.24	52.55
N217S	2.76 ± 0.19	20.4 ± 2.05	7.39
A193P	3.01 ± 0.33	16.04 ± 1.73	5.32
N160C	2.69 ± 0.23	25.93 ± 2.31	9.63
N217S/A193P/N160C	2.83 ± 0.42	21.23 ± 1.96	7.5
N217S/A193P/N160C/N122Y	2.33 ± 0.18	89.35 ± 3.19	38.35

Assays were performed using the synthetic peptide as substrate of AAPF in a concentration range of 100–600 mM at 40 °C in assay buffer containing 50 mM glycine-NaOH (pH 10.5). The different samples were incubated for 1 min at 40 °C. Results are mean values ± standard deviation from triplicate experiments

showed that hydrophobic interactions contribute 60 ± 4 % and hydrogen bonds contribute 40 ± 4 % to protein stability [14], which may be the reason for the enhanced thermostability of the N122Y mutant.

Kinetic parameters were determined using full term for AAPF (Table 5). All the amino acid substitutions, excepting N122Y, did not significantly change the apparent Michaelis constant (K_m) or catalytic turnover frequency (k_{cat}). The *B. licheniformis* keratinase showed a preference for aromatic or hydrophobic amino acid residues at the P1 position of synthetic *p*Na substrates [3], which interact with the S1 binding site. It is likely that the N217S, A193P, and N160C mutations are not close to the active site, and that the S1 binding site is sufficient to influence catalytic efficiency. However, the N122Y mutant enzyme displayed a 5.6-fold increased catalytic efficiency (k_{cat}/K_m) compared to the wild-type enzyme. This demonstrates the essential role of N122Y in the kinetic behavior of the *B. licheniformis* BBE11-1 keratinase. The increase in efficiency with regard to mutation N122Y can be ascribed mainly to the improved substrate affinity generated by this substitution by an aromatic residue [11].

As shown in Fig. 2b, N122Y has a relatively suitable distance (220Ser) to permit intramolecular interactions with the active site (Asp32, His63, 220Ser). This could be the reason for the changed catalytic efficiency. Finally, the corresponding N122Y/N217S/A193P/N160C quadruple mutant displayed a 4.1-fold increased catalytic efficiency (k_{cat}/K_m) as compared to the wild-type enzyme.

Conclusions

The PoPMuSiC algorithm was applied to predict amino acid substitutions to investigate the enhancement of the thermostability of the keratinase produced by *B. licheniformis* BBE11-1. Modification of subtilisin E and subtilisin BPN′ identified four beneficial substitutions (N122Y, N217S, A193P, and N160C). A corresponding quadruple mutant displayed synergistic or additive effects with an 8.6-fold increase in the $t_{1/2}$ value at 60 °C. The N122Y substitution also led to an approximately 5.6-fold increase in catalytic efficiency compared to that of the wild-type keratinase. Further insight and improvement of the enhanced thermostability of keratinase would be aided by molecular dynamics simulations.

Acknowledgments This project was financially supported by the National Natural Science Foundation of China (No. 30900013), the National High Technology Research and Development Program of China (863 Program, 2011AA100905), the National Key Technology R&D Program in the 12th Five year Plan of China (2011BAK10B03), the Program for Changjiang Scholars and Innovative Research Team in University (No. IRT1135), and the National High Technology Research and Development Program of China (863 Program, 2011AA100901). We are also grateful to Professor Byong Lee for his helpful discussion and revision.

References

1. Arnold K, Bordoli L, Kopp J, Schwede T (2006) The SWISS-MODEL workspace: a web-based environment for protein structure homology modelling. Bioinformatics 22:195–201
2. Barzegar A, Moosavi-Movahedi AA, Pedersen JZ, Miroliaei M (2009) Comparative thermostability of mesophilic and thermophilic alcohol dehydrogenases: stability-determining roles of proline residues and loop conformations. Enzyme Microbiol Technol 45:73–79
3. Brandelli A, Daroit DJ, Riffel A (2010) Biochemical features of microbial keratinases and their production and applications. Appl Microbiol Biotechnol 85:1735–1750
4. Brayan PN, Rollence ML, Pantoliano MW, Wood J, Finzel BC, Gilliland GL, Howard AJ, Poulos TL (2004) Proteases of enhanced stability: characteization of a thermostable variant of subtilisin. Proteins 1:326–334
5. Cabrita LD, Gilis D, Robertson AL, Dehouck Y, Rooman M, Bottomley SP (2007) Enhancing the stability and solubility of TEV protease using in silico design. Protein Sci 16:2360–2367
6. Chan MK, Mukund S, Kletzin A, Adams M, Rees DC (1995) Structure of a hyperthermophilic tungstopterin enzyme, aldehyde ferredoxin oxidoreductase. Science 267:1463
7. Dehouck Y, Kwasigroch JM, Gilis D, Rooman M (2011) PoPMuSiC 2.1: a web server for the estimation of protein stability changes upon mutation and sequence optimality. BMC Bioinformatics 12:151
8. Fisher SJ, Blakeley MP, Cianci M, McSweeney S, Helliwell JR (2012) Protonation-state determination in proteins using high-resolution X-ray crystallography: effects of resolution and completeness. Acta Crystallogr D 68:800–809
9. Gupta R, Sharma R, Beg QK (2012) Revisiting microbial keratinases: next generation proteases for sustainable biotechnology. Crit Rev Biotechnol. doi:10.3109/07388551.2012.685051
10. Gushterova A, Vasileva-Tonkova E, Dimova E, Nedkov P, Haertle T (2005) Keratinase production by newly isolated antarctic actinomycete strains. World J Microbiol Biotechnol 21:831–834

11. Jaouadi B, Aghajari N, Haser R, Bejar S (2010) Enhancement of the thermostability and the catalytic efficiency of *Bacillus pumilus* CBS protease by site-directed mutagenesis. Biochimie 92:360–369
12. Jaouadi B, Ellouz-Chaabouni S, Rhimi M, Bejar S (2008) Biochemical and molecular characterization of a detergent-stable serine alkaline protease from *Bacillus pumilus* CBS with high catalytic efficiency. Biochimie 90:1291–1305
13. Liu B, Zhang J, Li B, Liao X, Du G, Chen J (2012) Expression and characterization of extreme alkaline, oxidation-resistant keratinase from *Bacillus licheniformis* in recombinant *Bacillus subtilis* WB600 expression system and its application in wool fiber processing. World J Microbiol Biotechnol. doi:10.1007/s11274-012-1237-5
14. Pace CN, Fu H, Fryar KL, Landua J, Trevino SR, Shirley BA, Hendricks MM, Iimura S, Gajiwala K, Scholtz JM, Grimsley GR (2011) Contribution of hydrophobic interactions to protein stability. J Mol Biol 408:514–528
15. Pantoliano MW, Ladner RC, Bryan PN, Rollence ML, Wood JF, Poulos TL (1987) Protein engineering of subtilisin BPN′: enhanced stabilization through the introduction of two cysteines to form a disulfide bond. Biochemistry 26:2077–2082
16. Pantoliano MW, Whitlow M, Wood JF, Dodd SW, Hardman KD, Rollence ML, Bryan PN (1989) Large increases in general stability for subtilisin BPN′ through incremental changes in the free energy of unfolding. Biochemistry 28:7205–7213
17. Siezen RJ, Leunissen JA (1997) Subtilases: the superfamily of subtilisin-like serine proteases. Protein Sci 6:501–523
18. Takagi H, Hirai K, Wada M, Nakamori S (2000) Enhanced thermostability of the single-Cys mutant subtilisin E under oxidizing conditions. J Biochem 128:585–589
19. Tina KG, Bhadra R, Srinivasan N (2007) PIC: protein interactions calculator. Nucleic Acids Res 35:W473–W476
20. Watanabe K, Kitamura K, Suzuki Y (1996) Analysis of the critical sites for protein thermostabilization by proline substitution in oligo-1,6-glucosidase from Bacillus coagulans ATCC 7050 and the evolutionary consideration of proline residues. Appl Environ Microbiol 62:2066–2073
21. Williamson G, Vallejo J (1997) Chemical and thermal stability of ferulic acid esterase-III from *Aspergillus niger*. Int J Biol Macromol 21:163–167
22. Yamamura S, Morita Y, Hasan Q, Rao SR, Murakami Y, Yokoyama K, Tamiya E (2002) Characterization of a new keratin-degrading bacterium isolated from deer fur. J Biosci Bioeng 93:595–600
23. Yang DF, Wei YT, Huang RB (2007) Computer-aided design of the stability of pyruvate formate-lyase from *Escherichia coli* by site-directed mutagenesis. Biosci Biotech Biochem 71:746–753
24. Yang Y, Jiang L, Yang S, Zhu L, Wu Y, Li Z (2000) A mutant subtilisin E with enhanced thermostability. World J Microbiol Biotechnol 16:249–251
25. Zhang SB, Pei XQ, Wu ZL (2012) Multiple amino acid substitutions significantly improve the thermostability of feruloyl esterase A from *Aspergillus niger*. Bioresour Technol 117:140–147
26. Zhang SB, Wu ZL (2011) Identification of amino acid residues responsible for increased thermostability of feruloyl esterase A from *Aspergillus niger* using the PoPMuSiC algorithm. Bioresour Technol 102:2093–2096
27. Zhao H, Arnold FH (1999) Directed evolution converts subtilisin E into a functional equivalent of thermitase. Protein Eng 12:47–53
28. Zyprian E, Matzura H (1986) Characterization of signals promoting gene expression on the *Staphylococcus aureus* plasmid pUB110 and development of a gram-positive expression vector system. DNA 5:219–225